Reaction Chemistry & Engineering

ROYAL SOCIETY OF CHEMISTRY

PAPER

View Article Online
View Journal

Check for updates

Cite this: DOI: 10.1039/d5re00264h

A data-driven approach to the generalization of free radical polymerization kinetic models *via* automated flow chemistry

Amna Binte Asghar, Bo Zhang, Vianna F. Jafari and Tanja Junkers *

Systematic kinetic screening of chain transfer radical polymerizations was carried out using a continuous flow-based automated synthesis platform tailored for high-throughput screening of polymer reactions. The system features real-time online monitoring of monomer conversion and molecular weight distributions of residual polymers, enabling the generation of consistent, machine-readable kinetic datasets while minimizing user bias and experimental variability. A consistent dataset was obtained for the homopolymerization of butyl acrylate (BA), vinyl acetate (VAc) and methyl methacrylate (MMA) mediated by 1-dodecanethiol as the chain transfer agent, across a temperature range of 70 °C to 100 °C. A highly consistent dataset was obtained, allowing the determination of the respective chain transfer constants for each monomer at each temperature. On the test case of vinyl acetate polymerization, a generalized kinetic model for the rate of polymerization in the given parameter space was created *via* fitting of the individual overall kinetic coefficients for the rate of polymerization, obtained from 1st order kinetic data analysis. Bayesian optimization was then applied to predict which experimental conditions have the best potential to gradually improve the kinetic model, and interactive model improvement is demonstrated. This provides an important stepping stone for the development of self-driving labs that use databases to autonomously pick future experiments to carry out in order to improve their own data basis.

Received 19th June 2025,
Accepted 17th September 2025

DOI: 10.1039/d5re00264h

rsc.li/reaction-engineering

Published on 18 2025. Downloaded on 20-11-2025 00:38:19.

Introduction

The introduction of flow chemistry to chemistry labs, especially in the field of polymer chemistry, was for a long time seen as a mere engineering development.[1] Over the years, and with increasing success in the implementations of flow synthesis, the true potential of the methodology has been revealed[2] and many examples have been given where flow chemistry does not only offer an alternative route to chemical synthesis, but in which flow chemistry itself enables otherwise inaccessible chemistries.[3,4] In polymer synthesis, flow applications have opened access avenues to highly precise materials on scale.[5] *Via* telescoping, flow can give access to complex polymers at ease that in classical procedures would be very difficult to make.[6] Next to this, flow polymerization has significantly improved the reproducibility of polymer synthesis with impressive results for many different types of polymerizations.[6] As a further advantage, flow reactors, at least when surface to volume ratios are kept sufficiently high, are very close to ideal reactors. Consequently, flow reactors are by now an established technology found in many modern chemical synthesis laboratories.

Yet, recent years have brought a further revolution that elevates the field of flow chemistry to an even higher level. The ability to switch from manual control to automated operation in conjunction with online monitoring and other feedback systems has allowed for digitalization of flow synthesis and for the ability to perform smart self-optimization routines on reactions,[7] establishing flow chemistry as a high-throughput experimentation methodology.[8–13] In this context, also closed-loop self-optimizations have rapidly been realized, including multi-objective optimizations.[14] In polymer chemistry, algorithms have been developed that dynamically adjust flow processes to achieve a target molecular weights or precise monomer conversions—key factors in meaningful targeting of polymers.[10,15–17] This development frees significant time for researchers, allowing them to screen and improve reactions much faster than ever before. With this advantage in digital synthetic chemistry comes, however, also the need for better operation software, and more integrated algorithms that allow for swift decision making depending on circumstances, a task that is far from trivial.

Even with dedicated reaction optimization techniques like design of experiments (DoE) or Bayesian optimization,[18]

Polymer Reaction Design, School of Chemistry, Monash University, 19 Rainforest Walk, Building 23, Clayton, VIC 3800, Australia.
E-mail: tanja.junkers@monash.edu

Published on 18 2025. Downloaded on 20-11-2025 00:38:19.

optimizing reactions can still be time-consuming and inefficient due to the vast number of possible combinations that must be tested.[19,20] Further inefficiencies stem from the fact that most self-driving lab applications in the area work in isolation, and typically 'forget' the results of an optimization run once the objective(s) are achieved.[21,22] This challenge can be mitigated by integrating automation with machine-learning-based reaction optimization algorithms and with databases that store previously obtained data, making it available for future runs.[23,24] Yet, data does not only need to be generated and stored, it also needs to be automatically analyzed and curated in order to allow for good algorithm-based decision making. Further, once one moves from single optimizations to more generalized learning, more stringent data treatment becomes necessary, ranging from consistency checks to data aggregation.[25] The limit from which human comprehension still allows for rational decision making is reached quite quickly, and hence operations that to date are still often left to human operators, such as outlier detection, need to be generalized as well. Even if reactions are fully automated, errors can still occur, and machines need to be able to make distinctions between a good and a bad experimental result.[26] Building databases and introducing advanced machine learning that can harvest the benefit of vast (and partially scattered) data is an enormous task. In here, we demonstrate a stepping stone towards this goal. We show how the jump can be made from systematic screening of individual reactions to automated decision making towards continuous iterative model improvement. In this sense, decision making does not only refer to error detection, but primarily to the suggestion of new experiments to be performed with the aim of improving the overall machine learning model describing the reaction in question. The purpose here is not to optimize a specific synthesis outcome (a task that has been numerously demonstrated by now), but rather to generate comprehensive datasets that can ultimately provide a complete description of a particular reaction, and hence will allow to choose optimal conditions for any desired outcome instantly. To reach this aim, we make use of the automatic screening platform that we had previously described to screen controlled radical polymerization reactions.[9] In this previous work, we had demonstrated how automated screening removes the dependency of results from the human operator, and how consistent datasets can be created using such 'polymer synthesizer'. This is important as only if data is operator independent and virtually bias-free, generalizable results are obtainable. Further, in our previous work we demonstrated that the machine as used in here generates highly reproducible data which are very good agreement with offline analysis, hence validating the method. In here, we take the next step in using this device as a generic data generation machine that will itself propose the next experiment required to be carried out in order to improve a generalized kinetic model. Fig. 1 gives an overview over the approach that is taken. Based on a set of user-defined input variables data is obtained in high-throughput. The outcome of screenings is analyzed to provide a joint fit of all data. Optimization algorithms are then used to identify new reactions that will improve the joint fit, and the suggested experiments are conducted to improve the overall generalized model.

While we worked before on controlled radical polymerization, or more specifically, reversible-addition fragmentation chain-transfer (RAFT) polymerization, in this work, we took a step back to the simpler thiol-mediated chain transfer polymerization (CTP) (see Fig. 1c). CTP does not belong to the so-called reversible deactivation radical polymerizations, and does not allow for so-called livingness of chain growth. Yet, CTP still provides swift molar mass control of the resulting polymers (an essential characteristic to run flow polymerizations without the need for constant viscosity adjustment).[27] Most importantly though, CTP is in good approximation identical in kinetics to an uncontrolled free-radical polymerization (FRP),[28] and can hence serve as a model system to understand FRP kinetics, which is still the most abundant method used in industry to produce polymer products. Thus, by studying CTP in a broad range of thiol concentrations (which allows to extrapolate to zero thiol concentration) will later be able to predict free radical polymerizations to some extent as well. This in turn will allow to gain detailed insights in monomer reactivities and

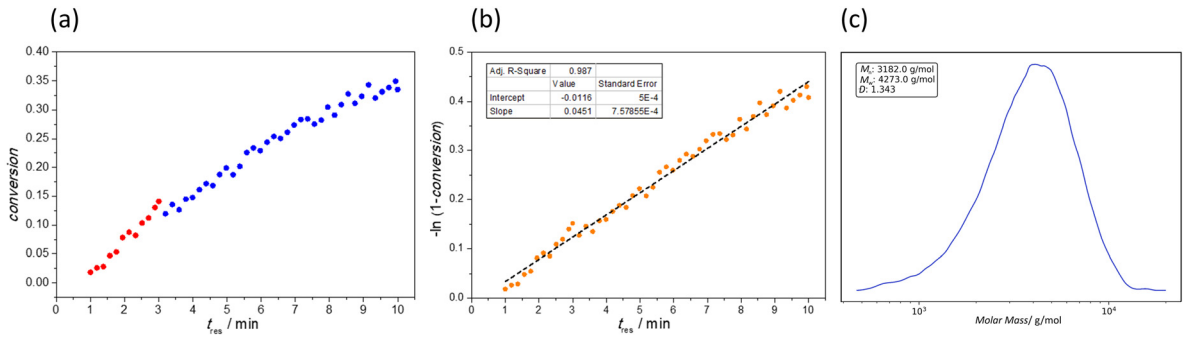

Fig. 1 Real-time monitoring plots from automatic screening of butyl acrylate at a c_T/c_M ratio 0.04 with 1-dodecanthiol at 80 °C. (a) Real-time monomer conversion against residence time; (b) first-order plot for the same data and (c) an example for a molar mass distribution obtained during the reaction.

 This journal is © The Royal Society of Chemistry 2025

Published on 18 2025. Downloaded on 20-11-2025 00:38:19.

the kinetics of the complex sub-reactions of the chain growth process.

Experimental

Materials

Butyl acrylate (BA, 99%, Merck), methyl methacrylate (MMA, 99%, Merck) and vinyl acetate (VAc, 99%, Merck) were deinhibited with a column of activated alumina before using. Azobis-isobutyronitrile (AIBN, 12 wt% in acetone, Sigma-Aldrich) was dried using a rotavap to remove acetone and recrystallized twice from methanol before use. 1-Dodecanthiol (98% Merck) and butyl acetate (BuOAc, 99% Merck) were used as received. HPLC-grade tetrahydrofuran (THF) was purchased from Thermo Scientific, and filtered before use for size exclusion chromatography.

Characterization

Inline NMR reaction monitoring was carried out with a low field benchtop 60 MHz NMR (Magritek, Spinsolve 1.19.0) *via* recording ^{1}H spectra (acquisition bandwidth 5 kHz: 83 ppm; acquisition time: 6.554 seconds; repletion time: 17 seconds). For data acquisition, the reaction monitor protocol was used, and a power shim was performed at the start and end of the day. Online SEC was performed on a custom-designed PSS system, operated by PSS WinGPC software. The SEC was equipped with a PSS SDV analytic column (50 × 8 mm), followed by one PSS SDV analytic 3.0 μm particle with porosity of 1000 Å (300 × 8 mm). The sample was analyzed *via* an evaporative light scattering detector (ELSD) ELS1300 using THF as eluent at 40 °C with a flow rate of 1 mL min^{-1}. The SEC system was calibrated with linear narrow polystyrene standards ranging from 474 to 7.5 × 10^{6} g mol^{-1} (K = 1.41 × 10^{-4} dL g^{-1} and α = 0.70).

General procedure of polymerization reaction screening

The high-throughput automated reaction screening platform was built by the Polymer Reaction Design group in a previous work.[9] A brief description of the platform is also provided in the supporting information of this contribution. In a typical procedure, the monomer (BA, MMA or VAc), chain transfer agent (1-dodecanthiol), initiator (AIBN) and solvent (BuOAc) were added to a 10 mL volumetric flask, then transferred to a glass vial and degassed with nitrogen for 5 minutes before use. Next, the reaction solution was transferred to a 10 mL gastight syringe (Trajan), purged with nitrogen at least three times, and placed in the holder of the syringe pump. The flow reactor was manually flushed with the solvent used in the reaction before each new reaction. After connecting the syringe to the flow reactor, the pump was started to make sure the block of the syringe pump was closed against the plunger of the syringe. Once the reaction solution was coming out from the syringe and moving in the tube, the pump was stopped manually, and the experiment was initiated *via* the automated platform's software. The recipes for all polymerization reactions are given in Tables S1–S9.

Results and discussion

Reaction screening

The general approach of this work is summarized in Scheme 1. The chain transfer polymerizations and monomers studied herein are given in Scheme 1c and d. 1b gives details of the experimental setup that we have used (unaltered from our previous work) and 1a outlines the automatic decision pathway taken by the algorithmic control of our polymer synthesizer. The polymer synthesizer as shown in Scheme 1b allows to carry out flow polymerizations. Computers take care of the entire reaction monitoring and based on preset time intervals, a so-called timesweep series experiment is performed.[29] In such experiment, the flow rate of the reaction is changed abruptly in different intervals, allowing for a very fast screening of the reaction with high time resolution. NMR and size exclusion chromatography (SEC) is used as online monitors, allowing to detect monomer conversion (the rate of polymerization) and the cumulative molecular weight obtained in the reaction at the same time. NMR in this case allows typically for second-scale time resolution while SEC gives results on the timescale of a few minutes. Since typically 2–3 timesweeps are consecutively carried out, a consistency check is built in the procedure, since only experiments in which the data from different sweeps match each other can be regarded as true results.

NMR spectra are measured directly on the reaction mixture, hence very broad spectra are obtained. Yet, integrals of peaks are still reliable and allow for a good determination of the reaction progress. An illustration of a representative spectrum from butyl acrylate polymerization is given in Fig. S1. Simultaneously, molecular weight parameters including number average molecular weight (M_n), weight average molecular weight (M_w), and dispersity ($Đ$) are obtained from SEC. A typical result from the timesweep experiments is shown in Fig. 1. These polymerization reactions can be considered as pseudo-first-order as confirmed from the first order plot in Fig. 1b (available for all 45 reactions in a data repository: **https://doi.org/10.26180/29208134**). CTPs typically yield polymers with a dispersity of around 2.[30,31] In our work, we often observed somewhat smaller dispersities in the range of 1.2–1.7, which can be explained by the use of an ELSD detector, which removes small oligomers. Consequently, especially for low molecular weight polymers, significant parts of the distribution are hence not considered, resulting in the lower apparent dispersity. As can be seen, polymerizations proceed in a controlled fashion with predictable increases in conversion as a function of residence time. This consistency is indicative of a well-behaved radical polymerization, supporting the reliability of CTP in continuous flow polymerizations.

Data from individual screenings are systematically stored in a designated folder as .csv files, updating every 18 seconds

Published on 18 2025. Downloaded on 20-11-2025 00:38:19.

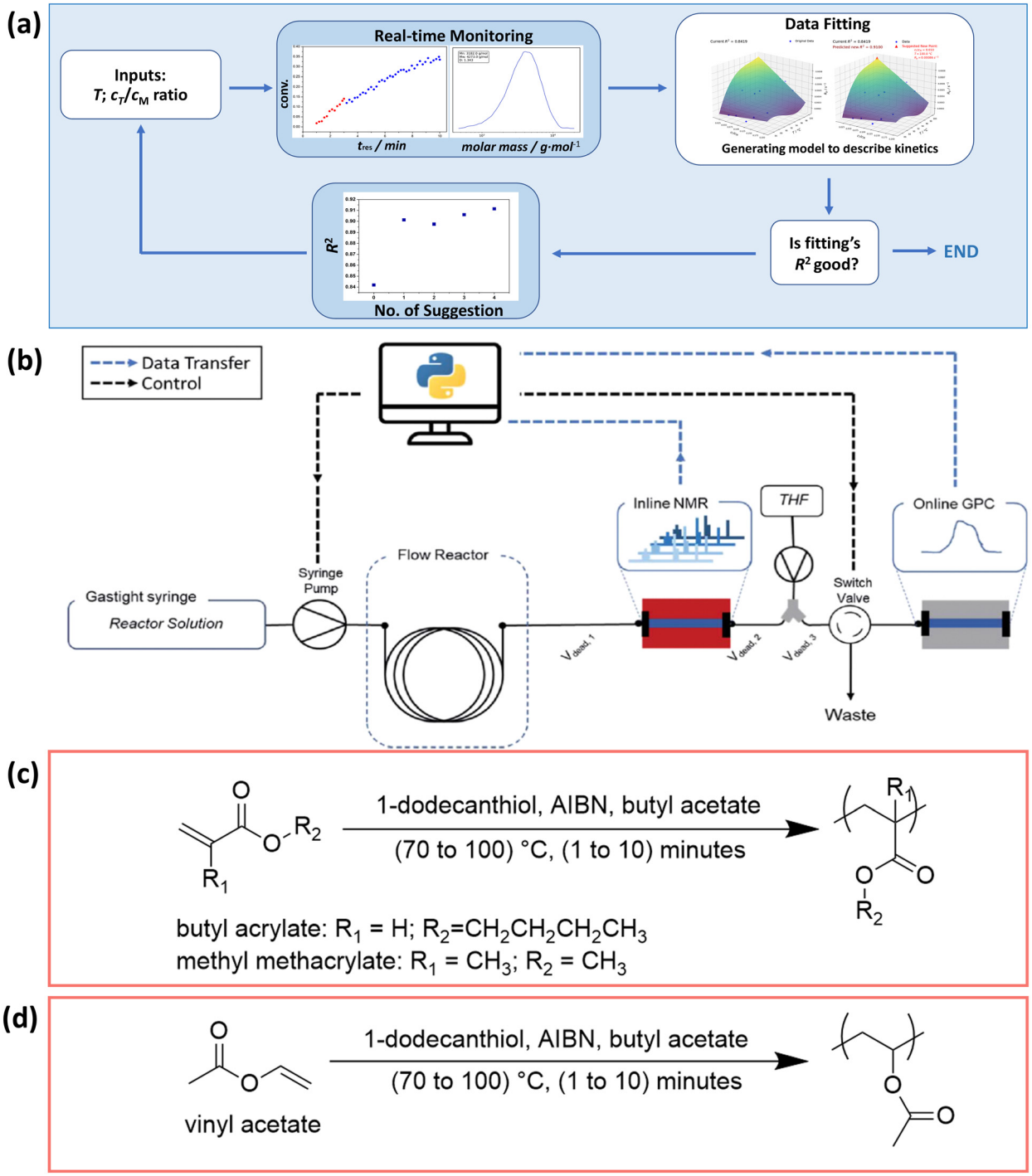

Scheme 1 (a) An overview of the structure of the data collecting, analysing and visualization; (b) high throughput automated reaction screening platform with inline analysis used; (c) chain transfer polymerizations screened in this work for monomer butyl acrylate and methyl methacrylate. (d) Chain transfer polymerizations screened in this work for monomer vinyl acetate.

throughout the experiments. This real-time monitoring approach enables the operator to promptly assess reactions and make corrective interventions before completion, averting potential failures. For the present work, we opted to screen CTPs involving three distinct monomers at temperatures ranging from 70 °C to 100 °C, in order to obtain a dataset with a broad scope. In a single reaction screening spanning 1 to 10 minutes of residence time, over 250 NMR spectra and 7 SEC chromatograms were acquired within 1.25 hours (including the dead volume). Extrapolating this to 50 different reaction conditions results in an estimated 12 500 NMR spectra and 350 SEC chromatograms. Despite the robust design of the platform and the reaction screening methodology, the collection of flawless data is not

This journal is © The Royal Society of Chemistry 2025

Published on 18 2025. Downloaded on 20-11-2025 00:38:19.

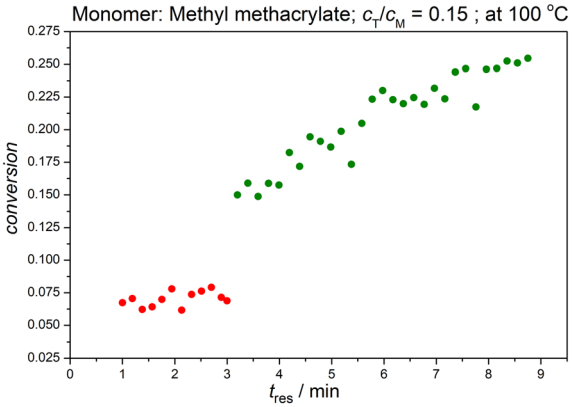

Fig. 2 Jump between timesweeps in vinyl acetate conversion screening at a c_T/c_M ratio of 0.15 with 1-dodecanthiol at 100 °C.

guaranteed. Before utilizing this substantial dataset for any kinetic study, it is thus imperative to validate the reliability of the data. Two primary types of deviations in NMR data can be observed on occasion, namely discrepancies between timesweeps (conversion jumping) or formal calculation of negative conversions, both stemming from the initiation of faulty experiments, brief software or hardware malfunctions or wrong choice of integration limits for the NMR spectra. NMR integrations can be adjusted if negative conversions are obtained, and hence our focus for error detection was primarily on addressing the issues related to the so-called timesweep jumps.

Fig. 2 illustrates such an instance of a jump. The jump can be observed between the first and second timesweep at 3 minutes residence time. In this case, a larger jump (more than 5% conversion) was observed between the two timesweeps, the first timesweep (1–3 minutes) was disregarded and the data from the second timesweep (3–10 minutes) was regarded as true data. Close inspection of Fig. 1a reveals also such a jump, yet at a rather insignificant level, and the joint constructed first order plot is nicely linear. For the data in Fig. 2 this would not be the case. These jumps originate from too high flow rates that hinder a proper evaluation of NMR intensities; if the flow rate is too high then magnetized material will leave the NMR detection volume before all spins have relaxed. In such case, the measured overall intensities can be wrong and hence conversion determination fails (as monomer and polymer have different relaxation times). Timesweeps covering a later time window will be less likely to suffer from such an effect, and can hence be assumed to be true.

Data-visualization

Controlling the molecular weight of polymers is crucial due to the profound impact on their physical and mechanical properties, tied to the length of polymer chains.[32,33] In the realm of FRP, chain transfer agents (CTA) are versatile tools to achieve chain length regulation in a simple and straightforward fashion while using cheap and available chemicals. The chain transfer constant, C_t, serves as a quantitative measure of a CTA's reactivity, defined as the ratio of the chain transfer to the propagation rate coefficient.[34] Notably, a higher C_t signifies a reduced need for a given concentration of the chain transfer agent to achieve specific molecular weight control.[34]

Expressed by the so-called Mayo equation, the instantaneous degree of polymerization (DP) exhibits a linear correlation with the ratio of CTA concentration (c_T) to monomer concentration (c_M), where C_t serves as the slope.[35] The Mayo eqn (1) allows for the simple prediction of expected molar masses in a chain transfer polymerization, and at the same time also offers an easy handle to determine the chain transfer constant.

$$\frac{1}{\mathrm{DP}_n} = C_t \frac{[\mathrm{CTA}]}{[\mathrm{M}]} + \frac{1+\alpha}{\mathrm{DP}_{n,0}} \quad (1)$$

In eqn (1), $\mathrm{DP}_{n,0}$ is the degree of polymerization in the absence of chain transfer agent (CTA), and α is the fraction of termination by disproportionation.

The Mayo equation yields the instantaneous DP_n at any given point in a polymerization, and is hence only strictly applicable at low monomer conversion.[36] As conversion increases, factors like rising viscosity, the gel (Trommsdorff) effect,[37] and the depletion of monomer relative to CTA concentration cause deviations from these assumptions and the accumulative obtained molar mass may slightly differ from the one at low conversion. These complexities make the Mayo equation less accurate at higher conversions, where the reaction kinetics become less predictable due to diffusion limitations[38] and increased viscosities.[37]

In here, we used the Mayo equation to test our data and in order to obtain chain transfer constants for the systems under investigation. For this matter, from all performed polymerization runs, the M_n of the lowest screened monomer conversion was selected and subjected to analysis following eqn (1). A reference Mayo plot for butyl acrylate and

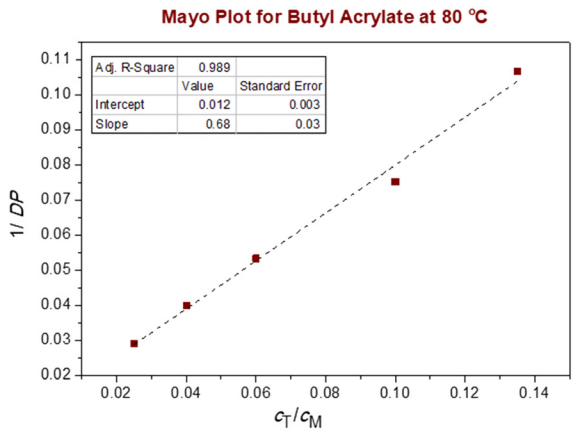

Fig. 3 Best fit of data to eqn (1) for 1-dodecanthiol-mediated polymerization of BA at 80 °C.

Published on 18 2025. Downloaded on 20-11-2025 00:38:19.

Table 1 Number average molecular weight obtained from dodecanthiol-mediated BA polymerization at 80 °C at various c_T/c_M ratios

c_T/c_M	M_n/g mol^{-1}	DP
0.025	4400	34
0.040	3200	25
0.060	2400	19
0.100	1700	13
0.135	1200	9

1-dodecanethiol at 80 °C is presented in Fig. 3, with the corresponding data summarized in Table 1. With increasing CTA concentrations relative to the monomer concentration, lower M_n and hence larger $1/DP_n$ are observed, following the linear relationship as predicted in eqn (1), with the slope of the best fit of the data yielding C_t. The corresponding plots and fits for all other polymerization are compiled and are available for reference in the supporting information (Fig. S2–S10). In the shown case here, C_t equals 0.682, a value largely in line with literature.[39] de la Fuente and López-Madruga (2001) reported $C_t \approx 1.51$–1.62 at 40–60 °C using Mayo and CLD methods. These values are substantially higher, yet these differences can stem from differences in solvent (benzene) and the overall or methodology used (batch *vs.* flow).

A summary of results is given in Table 2 for 1-dodecanthiol across various monomers at different temperatures. Notably, a generally increasing C_t is observed for higher temperatures, demonstrating that chain transfer is associated with a higher activation energy compared to the propagation rate coefficient, even if the screened temperature range is not sufficient to determine this activation energy gap accurately.[40] The increasing trend with temperature aligns with expectations, as the literature suggests that chain transfer constants for thiols increase with temperature due to enhanced reactivity of the S–H bond. For BA, the chain transfer constant increases with temperature, from 0.56 at 70 °C to 0.68 at 80 °C, and 0.77 at 90 °C. This trend suggests that the chain transfer reaction becomes more favorable as temperature rises. For MMA, the chain transfer constant also increases with temperature, from 0.56 at 80 °C to 0.63 at 90 °C, but remains constant at 0.63 from 90 °C to 100 °C. This plateau could indicate a balance between the activation energy of the chain transfer reaction and the propagation reaction, where further temperature increases do not significantly alter the ratio of their rate constants. The literature reports $C_t \sim 0.66$ for *n*-dodecanethiol with MMA at 60 °C,[41] only slightly higher than our 80–100 °C values of ~0.56–0.63. The discrepancy may arise from differences in experimental conditions (*e.g.*, solvent, initiator concentration) or measurement techniques (Mayo method *vs.* CLD) and can be considered a good match within error margins. Another source reports C_t values for MMA with *n*-dodecanethiol in the range of 0.5–0.7 at 60–70 °C, which aligns closely with the obtained values.[42] The values are also consistent with general trends for acrylates, where chain transfer constants with thiols are typically in the range of 0.5–1.0, depending on temperature and solvent conditions.

Table 2 Chain transfer constants of 1-dodecanthiol for three monomers at different temperatures obtained in this work

Chain transfer agent	Monomer	Temperature/°C	Chain transfer constant
1-Dodecanthiol	BA	70	0.56
		80	0.68
		90	0.77
	MMA	80	0.56
		90	0.63
		100	0.63
	VAc	85	0.47
		90	0.69
		100	0.71

For VAc, the comparison of the obtained apparent chain transfer with literature is less straight forward. Bon and coworkers pointed out that for monomer that are associated with transfer constants considerably larger than 1, erroneous results can be obtained using the Mayo equation.[43] In fact, the Mayo equation would underestimate the C_t in such case. Thus, the reported values for VAc in Table 2 should be taken with caution. However, the change in the apparent constant from 0.47 at 85 °C to 0.69 at 90 °C, and 0.71 at 100 °C shows nonetheless a significant shift in reactivity with temperature.

Regardless, the high quality of the linear relationships identified in the Mayo plots underpins the generally high quality and coherence of the dataset produced, which is more important than the actual chain transfer constants that have been determined in this high-throughput fashion. It should be noted that the C_t determination as such was not the aim of this study, and we only conducted the analysis since the data was available, and in order to test if linear plots are obtained. Monomers such as VAc would require further study to obtain more detailed and robust transfer constants.

Self-optimization

While the molar mass of a polymer made from chain transfer polymerization is well predictable as shown above, the rate of polymerization is not, and requires extensive kinetic study and modelling to make predictions. Theoretically, the overall reaction rate of free radical polymerization is determined by the initiation, propagation and termination rate. Chain transfer can also play a role, but is often assumed to be of minor influence with regard to the actual rate of polymerization. While initiation and propagation are relatively well understood in literature today, the diffusion-controlled nature of termination makes this reaction very complex and very difficult to predict, also because it can change over orders of magnitude during a reaction itself. As noted, a comprehensive description of the overall rate of polymerization requires detailed knowledge of each individual reaction step. Nevertheless, even with the best available data, accurately predicting the rate of a simple FRP

This journal is © The Royal Society of Chemistry 2025

Published on 18 2025. Downloaded on 20-11-2025 00:38:19.

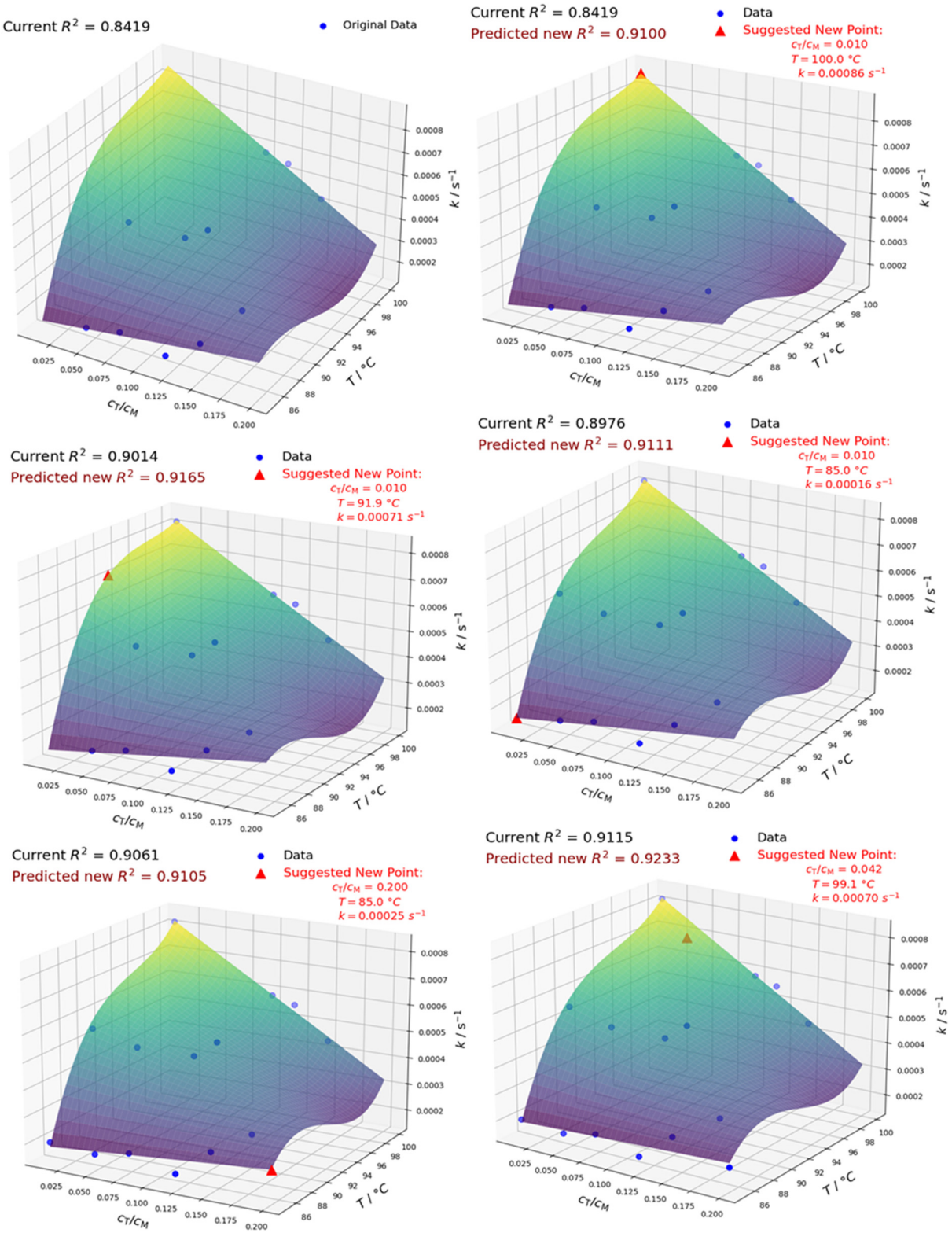

Fig. 4 3D Polynomial relationship between temperature (°C), rate (s^{-1}) and chain transfer agent to monomer concentration ratio (c_T/c_M) for vinyl acetate monomer and 1-dodecanthiol chain transfer agent. The current R^2 for each fitting depicts the R^2 at which the fitting is currently standing before making a suggestion. And predicted new R^2 means the expected R^2 if the suggested point is fully achieved. The suggested point is written in red ink and shows the new suggested data pair of c_T/c_M and T, and the expected/theoretical rate constant (k).

Published on 18 2025. Downloaded on 20-11-2025 00:38:19.

remains highly challenging. In practice, it is often more straightforward to determine the polymerization rate empirically. As shown in Fig. 1, FRPs typically show first-order kinetics in monomer concentration, since initiation and termination are in steady-state during polymerization. (REF) Thus, the overall rate is easily determined from timesweep data *via* the following equation:

$$\ln\left(\frac{M_t}{M_0}\right) = kt \tag{2}$$

In eqn (2), M_t is the concentration of monomer at residence time t, M_0 is the initial concentration of monomer and k is the overall reaction rate coefficient of free radical polymerization. Determining k for each reaction reduces the kinetic information for each polymerization to a single numerical value, giving access to a simplified data-driven exploration of the experimental parameter space. k is naturally a function of all individual rate coefficients as well as environmental factors. Human comprehension is limited when analyzing this complex function, yet machine-learning algorithms can statistically analyze the interdependencies, allowing to build empirical models that can then predict new reaction outcomes. To demonstrate this, we focused on the following vinyl acetate polymerization mediated by 1-dodecanthiol. Initially, 11 distinct experiments were conducted, with the detailed formulations for each reaction solution provided in Tables S7–S9. Subsequently, the data was treated as shown above, and k was determined for each polymerization, spanning a 3-dimensional parameter space (for concentrations and temperature, respectively, the set variable conditions of the polymerization. Fig. 4 shows how these parameter spaces look like. To generalize the parameter space, a customized polynomial fitting (third-order with respect to temperature as an approximation to its exponential relation with the rate of reaction and first-order with respect to c_T/c_M with an approximation of linear relation between concentration and rate of reaction for the first order kinetics) was performed.

The ensuing three-dimensional surface plot and fitting equation unsurprisingly illustrate the substantial impact of temperature on the reaction rate. What is more interesting is the relationship between the CTA concentration and the overall rate. While the radical transfer to the CTA is typically seen as fast and not rate determining, the obtained data reveals that the reaction rate of FRP is indeed distinctly influenced by the CTA concentration. This unexpected observation underscores the nuanced dynamics at play in the polymerization process, and also shows the level of detail that the empirical model can catch without trying to elucidate the underpinning individual rate coefficients.

In principle, the joint fit of the data provides a generalized model that is able to interpolate in the given parameter space for predictions of rate of polymerizations. However, given the relatively limited exploration of only 11 random experiments, there exists substantial potential for further refinement of the models. Indeed, using the original 3D surface fit in the upper left corner of Fig. 4, the R^2 value of the fit is 0.842, which indicates a good fit, but yet also indicates that the model can still be improved. Of course, one could from here choose further random experimental conditions to add to the dataset, which will certainly improve the goodness of the fit and thus the model. However, given the vast chemical parameter space, traditional statistical methods may prove insufficient for such optimization. Hence, a more efficient approach is warranted.

Thus, Bayesian optimization, a machine learning-driven self-optimizing algorithm, was employed to identify the most favorable parameter space for achieving the target outcomes and desired conditions.[44] Bayesian optimization constructs a probabilistic surrogate model, typically a Gaussian process, based on the given dataset and its polynomial fit. This surrogate model predicts the objective function across the parameter space while quantifying uncertainty in those predictions. Weaknesses in the fit—regions where the model is inaccurate or uncertain—are identified by analyzing areas with high predictive variance or significant deviations between the surrogate's predictions and observed data. BO employs an acquisition function, such as expected improvement or probability of improvement, to evaluate potential new data points. This function balances exploration (sampling uncertain regions) and exploitation (sampling regions likely to yield better outcomes), prioritizing points that are most likely to reduce uncertainty and improve the fit's accuracy. In our system, it was specifically adapted to seek the best trade-off among competing objectives, namely CTA concentration and temperature, employing the polynomial fitting equation to guide the selection of optimal experimental conditions. Leveraging the customized polynomial fitting equation and a generated predicted surrogate function, the algorithm identifies weaknesses in the given fit and suggests data points that are most likely to improve the overall fit. Thus, by iteratively suggesting new experiments, the polynomial fit of the dataset can be improved continuously, efficiently navigating the complex chemical parameter space and optimizing the experimental design for enhanced model performance. Fig. 4 shows the successive suggestion of new experiments to be carried out, and how they gradually improve the overal model.

Four strategically-suggested experiments were conducted for the FRP of vinyl acetate with 1-dodecanthiol, with the details of the reaction solutions provided in Tables S7–S9. As already mentioned, the initial dataset yielded an R^2 of 0.842. The Bayesian optimization algorithm suggested the first data point at c_T/c_M of 0.01 at 100 °C, suggesting that knowledge of this experimental outcome could potentially improve the R^2 for the fitting to 0.91. The predicted k for this suggested data point is 0.00086 s^{-1}. When the suggested experiment was conducted, this value was confirmed to be 0.00081 s^{-1}, hence while being roughly correct, slightly off from the prediction, nonetheless, this added datapoint increased the actual R^2 to 0.901, and hence also close to what the Bayesian optimization algorithm predicted. However, such

This journal is © The Royal Society of Chemistry 2025

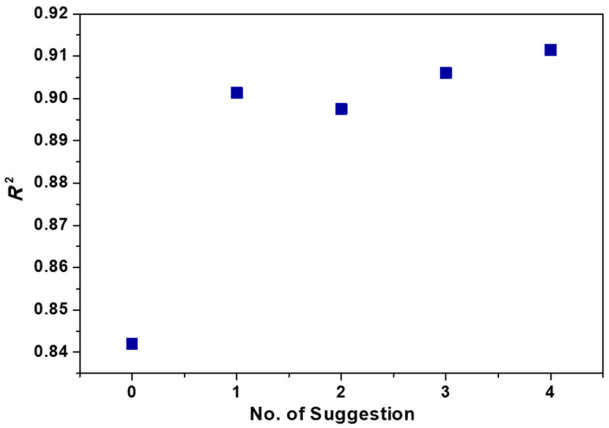

Fig. 5 R^2 of kinetic profile polynomial fitting after each suggestion given by the Bayesian optimization algorithm.

Published on 18 2025. Downloaded on 20-11-2025 00:38:19.

improvement is not always the case, and it can be seen with the next iteration that the suggested experiment resulted in a lower R^2 value. This indicates that the previous model was partly overfitted, and the decrease does not indicate a less good model as such. Generally, however, the model is expected to converge to higher R^2 with increasing numbers of iterations. Fig. 5 demonstrates this trend, showing the progression of R^2, advancing from 0.842 to just above 0.91. We carried out a few iterations here to demonstrate the concept, and seemingly for the given parameter space about 15 experiments have been sufficient to arrive at a relatively good model. It must be noted that R^2 will never reach unity, as experimental errors alone will always limit the model accuracy. The model in its most refined form successfully predicts now the expected rate of polymerization as a function of the c_T/c_M ratio and temperature T and has thus reached good generalization, as further significant improvements are not expected from more iterations. A comparison of the predicted and experimental k values is presented in Table S19. Thus, the goal was achieved to create a reliable general model for the prediction of reaction rates rather than optimizing the rate for a single set of conditions.

Conclusions

Using an automated kinetic screening platform that allows radical polymerizations to be followed with respect to conversion and molecular weight online, a significant dataset for chain transfer polymerizations of a series of monomers was generated. Fitting of molecular weight data to the Mayo equation allowed determination of the chain transfer constants at play for 1-dodecanethiol for different monomers and temperatures, showing the validity and good coherence of the obtained data. Further, the overall rates of polymerizations were investigated, and the hypothesis was tested if a generalized model can be created for the description of the rate of chain transfer polymerizations. Typically, in deterministic modelling, such a generalizable model would require intimate knowledge of number rate coefficients that underpin the entire reaction, a task that has not been achieved until today. Nonetheless, by using the given dataset, joint 3-dimensional fits could be made to describe the rate dependency on the parameter space, this being the chain transfer to monomer concentration ratio and the reaction temperature. It is then shown that Bayesian optimization can be used to increase the goodness and the predictivity of the models generated in this way iteratively.

This model lays the ground-work for self-optimizing machines. While at present the suggested new experiments still need to be initialized by a human operator, in future the entire process can be automated and new experiments be conducted without human interaction. Thus, this work introduces the concept for continuously learning and improving self-driving labs, showing the power that can be unfolded when automated chemical reactors will be connected with structural databases, allowing systems to continuously improve over time. We envision that such systems will likely reach higher predictivity and precision in polymerizations than classical modelling of reactions when the parameter space is gradually improved, and when databases are made more widely available, feeding more data in then continuously improves machine learning models.

Author contributions

Amna binte Asghar: conceptualization, investigation, methodology, validation, data curation, visualization and writing – original draft. Bo Zhang: validation and writing – original draft. Vianna F. Jafari: writing – review and editing. Tanja Junkers: conceptualization, methodology, validation, visualization, supervision, funding acquisition, project administration, resources, and writing – review and editing.

Conflicts of interest

The authors declare that they have no conflict of interest.

Data availability

Supplementary information: Recipes for presented polymerizations and characterization of obtained polymers. See DOI: **https://doi.org/10.1039/D5RE00264H**.

All data is available in a repository under **https://doi.org/10.26180/29208134**.

Acknowledgements

All authors wish to thank Monash University for general funding in the form of scholarships for A. B. A. and B. Z. Further, the authors are grateful for funding from the Australian Research Council *via* the discovery project DP240100120.

Published on 18 2025. Downloaded on 20-11-2025 00:38:19.

Notes and references

1 Y. Su, Y. Song and L. Xiang, in *Accounts on Sustainable Flow Chemistry*, ed. T. Noël and R. Luque, Springer International Publishing, Cham, 2020, pp. 147–190, DOI: **10.1007/978-3-030-36572-1_5**.
2 L. Capaldo, Z. Wen and T. Noël, *Chem. Sci.*, 2023, **14**, 4230–4247.
3 A. I. Alfano, J. García-Lacuna, O. M. Griffiths, S. V. Ley and M. Baumann, *Chem. Sci.*, 2024, **15**, 4618–4630.
4 P. Natho and R. Luisi, *Tetrahedron Green Chem*, 2023, **2**, 100015.
5 T. Junkers and B. Wenn, *React. Chem. Eng.*, 2016, **1**, 60–64.
6 N. Zaquen, M. Rubens, N. Corrigan, J. Xu, P. B. Zetterlund, C. Boyer and T. Junkers, *Prog. Polym. Sci.*, 2020, **107**, 101256.
7 A. Slattery, Z. Wen, P. Tenblad, J. Sanjose-Orduna, D. Pintossi, T. den Hartog and T. Noel, *Science*, 2024, **383**, eadj1817.
8 J. J. Haven and T. Junkers, *Chim. Oggi – Chem. Today*, 2018, **36**, 42–44.
9 J. Van Herck, I. Abeysekera, A.-L. Buckinx, K. Cai, J. Hooker, K. Thakur, E. Van de Reydt, P.-J. Voorter, D. Wyers and T. Junkers, *Digital Discovery*, 2022, **1**, 519–526.
10 M. Rubens, J. H. Vrijsen, J. Laun and T. Junkers, *Angew. Chem., Int. Ed.*, 2019, **58**, 3183–3187.
11 M. Rubens, J. Van Herck and T. Junkers, *ACS Macro Lett.*, 2019, **8**, 1437–1441.
12 D. C. Fabry, E. Sugiono and M. Rueping, *React. Chem. Eng.*, 2016, **1**, 129–133.
13 C. Mateos, M. J. Nieves-Remacha and J. A. Rincón, *React. Chem. Eng.*, 2019, **4**, 1536–1544.
14 A. M. Schweidtmann, A. D. Clayton, N. Holmes, E. Bradford, R. A. Bourne and A. A. Lapkin, *Chem. Eng. J.*, 2018, **352**, 277–282.
15 S. T. Knox, K. E. Wu, N. Islam, R. O'Connell, P. M. Pittaway, K. E. Chingono, J. Oyekan, G. Panoutsos, T. W. Chamberlain, R. A. Bourne and N. J. Warren, *Polym. Chem.*, 2025, **16**, 1355–1364.
16 Y. Gu, P. Lin, C. Zhou and M. Chen, *Sci. China: Chem.*, 2021, **64**, 1039–1046.
17 J. D. Tan, B. Ramalingam, S. L. Wong, J. J. W. Cheng, Y.-F. Lim, V. Chellappan, S. A. Khan, J. Kumar and K. Hippalgaonkar, *J. Chem. Inf. Model.*, 2023, **63**, 4560–4573.
18 B. J. Shields, J. Stevens, J. Li, M. Parasram, F. Damani, J. I. M. Alvarado, J. M. Janey, R. P. Adams and A. G. Doyle, *Nature*, 2021, **590**, 89–96.
19 S. A. Weissman and N. G. Anderson, *Org. Process Res. Dev.*, 2015, **19**, 1605–1633.
20 M. I. Jeraal, S. Sung and A. A. Lapkin, *Chem.: Methods*, 2021, **1**, 71–77.
21 R. J. Hickman, J. Ruža, H. Tribukait, L. M. Roch and A. García-Durán, *React. Chem. Eng.*, 2023, **8**, 2284–2296.
22 F. Häse, L. M. Roch and A. Aspuru-Guzik, *Trends Chem.*, 2019, **1**, 282–291.
23 J. P. McMullen and J. A. Jurica, *React. Chem. Eng.*, 2024, **9**, 2160–2170.
24 L.-Y. Chen and Y.-P. Li, 2024, DOI: **10.26434/chemrxiv-2024-wt75q-v2**.
25 E. Bhardwaj, H. Gujral, S. Wu, C. Zogheib, T. Maharaj and C. Becker, presented in part at the *Proceedings of the 2024 ACM Conference on Fairness, Accountability, and Transparency*, Rio de Janeiro, Brazil, 2024.
26 F. Gusev, B. C. Kline, R. Quinn, A. Xu, B. Smith, B. Frezza and O. Isayev, *ChemRxiv*, 2025, preprint, DOI: **10.26434/chemrxiv-2025-7ggzl**.
27 J. P. Lutz, M. D. Hannigan and A. J. McNeil, *Coord. Chem. Rev.*, 2018, **376**, 225–247.
28 N. Moghadam, S. Liu, S. Srinivasan, M. C. Grady, A. M. Rappe and M. Soroush, *Ind. Eng. Chem. Res.*, 2015, **54**, 4148–4165.
29 J. Van Herck and T. Junkers, *Chem.: Methods*, 2022, **2**, e202100090.
30 G. Odian, *Principles_of_Polymerization*, 4th edn, 2004.
31 A. Bagheri, S. Boniface and C. M. Fellows, *Chem. Teach. Int.*, 2021, **3**, 19–32.
32 T. Q. Nguyen and H. H. Kausch, in *Mechanical Properties and Testing of Polymers: An A–Z Reference*, ed. G. M. Swallowe, Springer Netherlands, Dordrecht, 1999, pp. 143–150, DOI: **10.1007/978-94-015-9231-4_32**.
33 G. Vaganov, M. Simonova, M. Romasheva, A. Didenko, E. Popova, E. Ivan'kova, A. Kamalov, V. Elokhovskiy, V. Vaganov, A. Filippov and V. Yudin, *Polymers*, 2023, **15**(13), 2922.
34 J. P. A. Heuts and N. M. B. Smeets, *Polym. Chem.*, 2011, **2**, 2407–2423.
35 E. L. M. José Luis De La Fuente, 2000.
36 S. Chi, Y. Yu and M. Zhang, *Polymer*, 2022, **256**, 125181.
37 J. M. Nölle, S. Primpke, K. Müllen, P. Vana and D. Wöll, *Polym. Chem.*, 2016, **7**, 4100–4105.
38 B. S. Casey, M. F. Mills, D. F. Sangster, R. G. Gilbert and D. H. Napper, *Macromolecules*, 1992, **25**, 7063–7065.
39 J. L. de la Fuente and E. López Madruga, *Macromol. Chem. Phys.*, 2001, **202**, 375–381.
40 In *Studies in Physical and Theoretical Chemistry*, ed. A. K. Galwey and M. E. Brown, Elsevier, 1999, vol. 86, pp. 117–138.
41 J. L. De La Fuente and E. L. Madruga, *J. Polym. Sci., Part A: Polym. Chem.*, 2000, **38**, 170–178.
42 O. Çetinkaya, G. Demirci and P. Mergo, *Opt. Mater.*, 2017, **70**, 25–30.
43 M. K. Donald and S. A. F. Bon, *Polym. Chem.*, 2020, **11**, 4281–4289.
44 O. Schilter, D. P. Gutierrez, L. M. Folkmann, A. Castrogiovanni, A. García-Durán, F. Zipoli, L. M. Roch and T. Laino, *Chem. Sci.*, 2024, **15**, 7732–7741.

 This journal is © The Royal Society of Chemistry 2025